14. R. I. Nigmatulin, Principles of the Mechanics of Heterogeneous Media [in Russian], Moscow (1978).
15. V. I. Timoshenko, Inzh.-fiz. Zh., 45, No. 2, 226-231 (1983).

NUMERICAL SIMULATION OF THE FLOW OF A SUPERSONIC STREAM OF VISCOUS COMPRESSIBLE GAS OVER A CAVITY

I. A. Graur, T. G. Elizarova, and B. N. Chetverushkin

Numerical simulation of the flow of a supersonic stream of viscous, compressible, heat-conducting gas over a cavity is carried out on the basis of kinetically consistent difference schemes. Different types of flow ("open" and "closed" cavities) are considered, the heat fluxes to the walls of the recess are determined, and a nonsteady regime of flow over a cavity is simulated. The results obtained are compared with known experimental relationships.

1. Introduction

Experimentally observed detached flows in recesses, over which a supersonic stream of viscous gas flows, have both a steady and a nonsteady character [1-5]. The types of such flows have been classified in [5]. Numerical simulation of these flows is urgently needed for practical applications of problems of computational hydrodynamics, the complexity of which is due to the need for simultaneous allowance for the region of inviscid flow and for viscous effects within the boundary layer. Let us cite several of the most typical examples of the calculation of such flows. Conjugation of solutions for the compressible boundary layer above the recess, for the compressible Navier—Stokes equation within the recess, and for inviscid flow above the recess outside of the boundary layer has been used in [6] to calculate steady detached flow in a cavity. In such an approach, however, an iterative process cannot be constructed to join the solutions for calculating nonsteady flows, and in that case it is natural to use the complete Navier—Stokes equations for numerical simulation. In [3], in particular, the averaged Navier—Stokes equations were used in combination with McCormack's method, and in [7] the method of splitting with respect ot physical processes and spatial variables was used. To calculate pulsation flows in the model of an ideal gas, which seems simpler from the standpoint of practical computation, periodic variations of the parameters at the entrance boundary must be specified to excite oscillations in the cavity [8].

In the present paper, which is a continuation of [9], we carry out a series of calculations of supersonic flow over cavities by a stream of viscous compressible gas on the basis of kinetically consistent difference schemes (KCDSs) with corrections [10]. Although the flow in a cavity has a three-dimensional character, as noted experimentally, the two-dimensional formulation of the problem has been considered to clarify the main features of that flow and reduce the volume of calculations. Laminar flow regimes have been investigated. In the calculations we varied the geometrical dimensions of the recesses and studied flow in cavities of two different types: "open" and "closed." The heat fluxes to the cavity walls were determined in the case of isothermal boundary conditions. The pulsation regime of flow was simulated for an adiabatic cavity of the open type. In this case, in contrast to [8], we did not have to specify perturbations of the parameters at the entrance boundary to excite the oscillations. The results of the calculations have been compared with the known experimental data [1, 5]. In the case of pulsation flow, the results were compared with known data of natural experiments [2, 4] and with analytic functions [3].

2. Statement of the Problem

We write the KCDS, with corrections for the two-dimensional case, in the (x, y) geometry (the system is written in dimensionless form):

$$\rho_t + (\rho u)_{\underset{x}{0}} + (\rho v)_{\underset{y}{0}} = \left[\frac{h_x}{2c}(\rho u^2 + p)_{\bar{x}}\right]_x + \left[\frac{h_y}{2c}(\rho v^2 + p)_{\bar{y}}\right]_y,$$

$$(\rho u)_t + (\rho u^2 + p)_{\underset{x}{0}} + (\rho u v)_{\underset{y}{0}} = \left[\frac{h_x}{2c}(\rho u^3 + 3pu)_{\bar{x}}\right]_x +$$

$$+ \left[\frac{h_y}{2c}(\rho u v^2)_{\bar{y}}\right]_y + \frac{1}{\mathrm{Re}}\left[\frac{4}{3}(\mu u_{\bar{x}})_x + (\mu u_{\bar{y}})_y\right],$$

$$(\rho v)_t + (\rho u v)_{\underset{x}{0}} + (\rho v^2 + p)_{\underset{y}{0}} = \left[\frac{h_x}{2c}(\rho u^2 v)_{\bar{x}}\right]_x +$$

(1)

$$+ \left[\frac{h_y}{2c}(\rho v^3 + 3pv)_{\bar{y}}\right]_y + \frac{1}{\mathrm{Re}}\left[(\mu v_{\bar{x}})_x + \frac{4}{3}(\mu v_{\bar{y}})_y\right],$$

$$E_t + [u(E+p)]_{\underset{x}{0}} + [v(E+p)]_{\underset{y}{0}} = \left[\frac{h_x}{2c}\left(u^2\left(E + \frac{5}{2}p\right)\right)_{\bar{x}}\right]_x +$$

$$+ \left[\frac{h_y}{2c}\left(v^2\left(E + \frac{5}{2}p\right)\right)_{\bar{y}}\right]_y + \left[\frac{h_x}{2c}\frac{2p_{\bar{x}}}{\rho(\gamma-1)}\right]_x + \left[\frac{h_y}{2c}\frac{2p_{\bar{y}}}{\rho(\gamma-1)}\right]_y +$$

$$+ \frac{1}{\mathrm{Re}}\left[\left(\mu\left(\frac{4}{3}\frac{u^2}{2} + \frac{v^2}{2}\right)_{\bar{x}}\right)_x + \left(\mu\left(\frac{u^2}{2} + \frac{4}{3}\frac{v^2}{2}\right)_{\bar{y}}\right)_y\right] + \frac{1}{\mathrm{Re}}\frac{\gamma}{\mathrm{Pr}}[(\mu \varepsilon_{\bar{x}})_x + (\mu \varepsilon_{\bar{y}})_y],$$

$$p = (\gamma - 1)\rho \varepsilon, \quad \gamma = c_p/c_v.$$

(2)

The central, left-hand, and right-hand difference derivatives with respect to x (and to y) and denoted by the indices $\overset{0}{x}$, $\bar{x}$, x ($\overset{0}{y}$, $\bar{y}$, y), respectively.

The system (1) was made dimensionless as follows:

$$x = \tilde{x}L, \quad y = \tilde{y}L, \quad \rho = \tilde{\rho}\rho_\infty, \quad u = \tilde{u}u_\infty, \quad v = \tilde{v}u_\infty,$$

$$c = \tilde{c}u_\infty, \quad p = \tilde{p}\rho_\infty u_\infty^2, \quad \varepsilon = \tilde{\varepsilon}u_\infty^2, \quad \mu = \tilde{\mu}\mu_\infty,$$

$$t = \tilde{t}L/u_\infty, \quad \mathrm{Re} = \rho_\infty u_\infty L/\mu_\infty.$$

The boundary conditions u = v = 0 and ε_w = const or $\partial\varepsilon/\partial n = 0$ and $\partial p/\partial n = 0$ at the cavity walls were specified for the system (1).

The geometry of the calculation region is shown in Fig. 1. A laminar boundary layer of thickness δ was specified at the left-hand entrance boundary of the region. The distribution of the horizontal velocity component in the boundary layer was determined from the equation [11]

$$\frac{u}{u_\infty} = \frac{3}{2}y/\delta - \frac{1}{2}(y/\delta)^3.$$

The vertical velocity component was assumed to equal zero or was determined from the equation

$$\frac{v}{u_\infty} = 2.32\left(\frac{\mu_\infty}{\rho_\infty u_\infty x}\right)^{1/2}\left(\frac{3}{4}(y/\delta)^2 - \frac{3}{8}(y/\delta)^4\right).$$

The temperature distribution in the boundary layer was specified in accordance with the Grocco integral [11],

$$\frac{T}{T_\infty} = 1 + \frac{T_e - T_\infty}{T_\infty}[1 - (u/u_\infty)^2] + \frac{T_w - T_e}{T_\infty}(1 - u/u_\infty),$$

where $T_e = T_\infty\left(1 + r\frac{\gamma-1}{2}M_\infty\right)^2$ is the equilibrium wall temperature; r is the coefficient of restitution, equal to $(\mathrm{Pr})^{1/2}$ for laminar flow; M_∞ is the Mach number in the undisturbed oncoming stream.

The pressure was assumed to be constant across the boundary layer. The density was de-
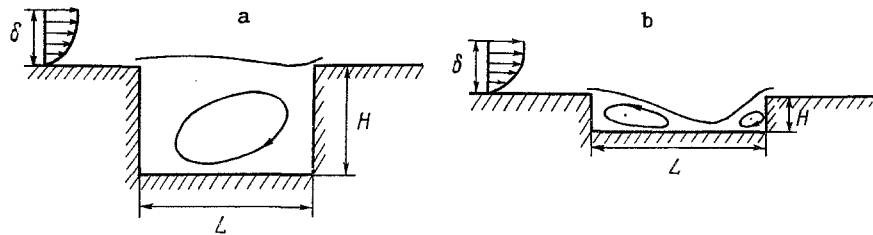
Fig. 1. General flow pattern and geometry of the calcula-
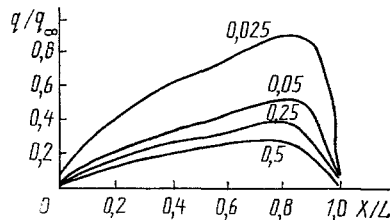tion region: a) open cavity; b) closed cavity.

Fig. 2. Heat fluxes at the bottom of the
cavity, normalized to the heat flux at the
entrance boundary, q/q_∞ (0.5, 0.25, 0.05,
and 0.025 are the dimensionless depths of
the cavities); Re = $1.0 \cdot 10^3$, M = 1.05.

termined from the known pressure and temperature using (2). The upper boundary of the cal-
culation region was located a distance of about five or six times the thickness of the bound-
ary layer from the horizontal surface, i.e., where the derivatives of the gas-dynamic parame-
ters normal to the flow are small. The open right-hand boundary of the region lay at a dis-
tance equal to the length of the recess, where the flow disturbances produced by the cavity
are small, according to the data of [3, 5]. The first derivatives of all of the gas-dynamic
parameters with respect to the normal to the boundary were assumed to vanish at the open
boundaries described above.

The temperature dependence of viscosity was given by a power-law approximation of the
Sutherland equation [11], $\mu/\mu_\infty = (\varepsilon/\varepsilon_\infty)^\omega$, using ω = 0.75 for the exponent. The heat flux
to the wall was determined from the equation

$$q = \gamma/(\mathrm{Pr\,Re})\mu \,(\partial \varepsilon/\partial y|_{y=0}. \tag{3}$$

The following initial conditions were used in the calculations: a boundary layer of
thickness δ was specified everywhere above the recess. Inside the recess the gas velocity
was assumed to equal zero, and the temperature and pressure equalled the respective values
in the undisturbed oncoming stream. The calculations were carried out by the scheme (1)
using the establishment method.

Below we briefly give the main results of numerical simulation of the problem of flow
over a cavity in the above formulation.

3. Results of Numerical Calculations

Rectangular Cavity. Flow over a rectangular cavity (H/L = 0.5) was considered. The
Mach number in the undisturbed oncoming stream was M = 1.3. The Reynolds number, calculated
from the cavity length L, was Re = $1.2 \cdot 10^3$. The Prandtl number was Pr = 0.71 and the ini-
tial thickness of the boundary layer was δ/H = 0.23. The cavity walls were isothermal, T_w =
$0.2T_\infty$.

A general diagram of the flow and the geometry of the calculation region are shown in
Fig. 1a. The flow pattern obtained had the following features. The boundary layer, having
detached from the left-hand edge of the cavity, completely covers the recess and is reat-
tached, having become somewhat thicker, near its right-hand corner. In the interior of the
cavity one large, elongated vortex is formed, shifted relative to the geometrical center of
the cavity toward its right-hand wall. The established type of flow is consistent with ex-
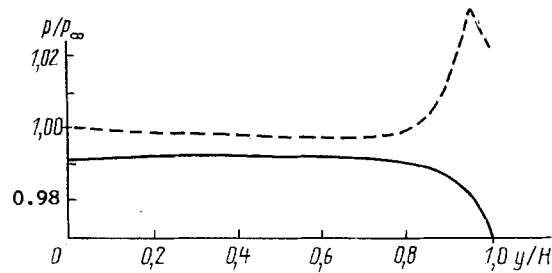perimental data obtained in [5]. There it was indicated that cavities having dimensions 0.1 $\le$

Fig. 3. Pressure p/p_∞ at the cavity walls
(dashed line: pressure at the right-hand
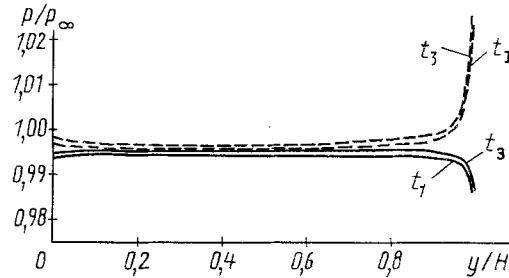wall; solid line: at the left-hand wall);
$Re = 1.0\cdot10^3$, $M = 1.05$.

Fig. 4. Pressure p/p_∞ at the cavity walls
(dashed lines: pressure at the right-hand
wall; solid lines: at the left-hand wall)
for the times $t_1 = 260$ and $t_3 = 270$; $Re_H =$
$3.3\cdot10^4$, $M = 1.3$.

$H/L \leq$ belong to the type of so-called shallow open cavities, the flow in which is typified by the formation of one vortex in the cavity, shifted downstream, and attachment of the detached boundary layer at the right-hand edge of the cavity.

The heat fluxes at the bottom of the cavity and at its walls were calculated from Eq. (3) for the given problem. The maximum heat fluxes are in the region near the right-hand corner of the cavity, i.e., in the region where the detached boundary layer is reattached. The largest flux at the right-hand wall, normalized to the value in the oncoming stream, is 1.2, and the maximum flux at the bottom is 0.2.

Cavities of Different Depths. On the basis of a solution of the system (1), we simulated the flow in cavities of different depths. The depths were chosen so that we could analyze two types of flow: in "open" and "closed" cavities. The Mach number was $M = 1.05$ and the thickness of the oncoming boundary layer was $\delta/L = 0.116$. The walls of the recess were isothermal: $T_w = 0.2T_\infty$. We analyzed cavities with depths $H/L = 0.5$, 0.25, 0.05, and 0.025.

A typical feature of flow over a cavity of depth $H/L = 0.5$ is the formation of one large vortex in the interior of the cavity and the reattachment of the detached boundary layer near the right-hand edge of the cavity. This is a "shallow open cavity" in the classification of [5]. The heat fluxes at the vertical walls increase monotonically and have maxima near the right-hand and left-hand outer corners of the cavity. The maximum flux at the right-hand wall is almost 1.7 times larger than the corresponding flux at the left-hand wall, which is related to the attachment of the stream in the vicinity of the upper right-hand corner of the cavity. A graph of the flux at the bottom is shown in Fig. 2, marked by the number 0.5. The largest flux corresponds to the center of the vortex formed in the cavity.

The flow established in a cavity of depth $H/L = 0.25$ is similar to the flow described above. The heat flux at the bottom is given in Fig. 2, marked by the number 0.25.

We then considered flow over a cavity of depth $H/L = 0.05$. One large vortex near the left-hand wall and a small vortex of opposite circulation in the lower right-hand corner were formed in the cavity, and the detached boundary layer was attached at the bottom of the

recess. According to the data of [5], a cavity with such a geometry is of the "shallow closed" type, the flow in which is characterized by the formation of two detached regions, one of which is formed behind the step down from the stream and the second ahead of the step up into the stream, as well as by the presence of two vortices of different sizes near the right-hand and left-hand corners of the cavity (see Fig. 1b). The pressure at the left-hand vertical wall of the cavity has the form typical of flow over a down step: the pressure minimum is located near the upper left-hand corner of the cavity, from which the stream detaches, and it is lower than p_∞ (Fig. 3, solid line). The pressure at the right-hand vertical wall (Fig. 3, dashed line) is typical of flow over a step up into the stream: the pressure maximum is reached somewhat below the upper right-hand corner of the cavity, near the attachment point of the stream. For a cavity of the open type, the pressure distribution at the right-hand wall is somewhat different (Fig. 4, dashed lines): the pressure maximum lies directly at the right-hand corner of the cavity, rather than below that corner. In Fig. 5 we give graphs of the pressure distribution over the bottom of the cavity for flow in cavities of the open (H/L = 0.5) and closed (H/L = 0.05) types. The character of the pressure variation is consistent with experimental data [1]. The pressure over the bottom of an open cavity is almost constant and has a slight minimum near the left-hand wall. A closed cavity is characterized by a rise in pressure over the entire length of the recess. The heat flux at the bottom of this cavity is shown in Fig. 2, marked by the number 0.05.

The character of the flow over a cavity of depth H/L = 0.025 is similar to that for H/L = 0.05. The main features of the flow are the formation of two vortices of different sizes in the cavity and the attachment of the stream at the bottom of the recess. The heat fluxes at the vertical walls of the cavity have the same monotonically increasing character as for H/L = 0.5. Their maximum values become very close (differing by a few percent), however. The heat flux at the bottom is given in Fig. 2, marked by the number 0.025.

Thus, upon a decrease in the depth of the cavity from H/L = 0.25 to H/L = 0.05, the type of flow changes, i.e., from flow in an open cavity to that in a closed cavity. As the depth of the cavity varies from H/L = 0.5 to H/L = 0.025, the fluxes at the vertical walls decrease, and from differing considerably (the flux at the right-hand wall is about twice the flux at the left-hand wall for H/L = 0.5), they become almost equal (for H/L = 0.025). The decrease in the depth of the cavity changes the flux at the bottom, the flux for H/L = 0.025 being more than four times that for H/L = 0.5. The character of the pressure distribution over the bottom and walls of the recess changes with a change in the depth of the cavity.

Oscillatory Flow Regime. Supersonic flow (M = 1.35) over a rectangular recess (H/L = 0.5) was considered. The walls of the recess were adiabatic. The initial thickness of the boundary layer was $\delta/H = 0.046$. The Reynolds number, calculated from the depth of the recess, was $Re_H = 3.3 \cdot 10^4$. This problem was calculated on two grids, (67 × 62) and (91 × 83), bunched in x and y, with minimum steps in x and y of $h^x_{1min} = 6 \cdot 10^{-2}$, $h^y_{1min} = 2 \cdot 10^{-2}$ and $h^x_{2min} = 2 \cdot 10^{-2}$, $h^y_{2min} = 1 \cdot 10^{-2}$, respectively. The results of the calculations on these two grids almost coincide.

According to the experimental data generalized in [3], the nonsteady shear layer formed by detachment from the front edge of the cavity is the main reason for the development of pulsations. For pulsations to develop it is also necessary that the cavity be fairly long compared with the thickness of the boundary layer, $L > 2\pi\delta$, and that the Mach number satisfy
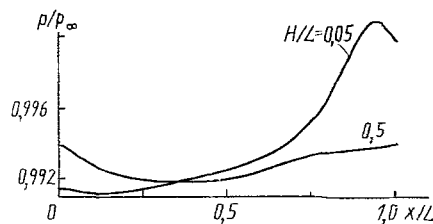

Fig. 5. Pressure p/p_∞ at the bottom of the cavity. The numbers 0.5 and 0.05 denote the dimensionless depth of the cavity; Re = 1.0· 10^3, M = 1.05.
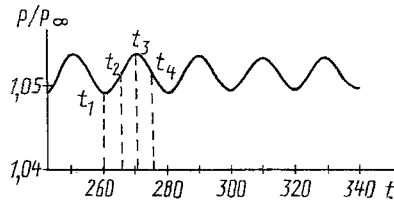
Fig. 6. Variation of the pressure p/p_∞ at the right-hand wall of the cavity as a function of time t; $R_{eH} = 3.3 \cdot 10^4$, M = 1.3.
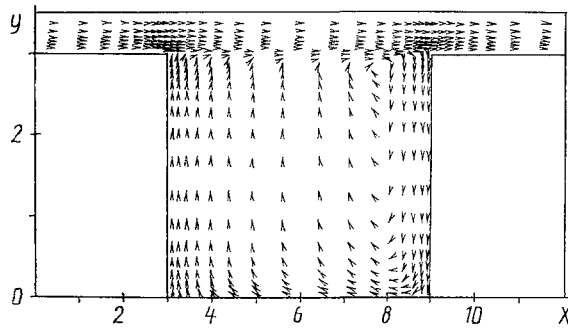

Fig. 7. Direction of flow velocity; $Re_H = 3.3 \cdot 10^4$, M = 1.3.

the relation M < 2.5. These conditions are satisfied for the problem formulated above. The gas stream impinging on the cavity excited low-amplitude pressure pulsations at the bottom of the recess and at its walls (according to the data of [4], the amplitude of the pulsations must be about 1%). The mechanism of formation of the pulsations has been described in detail in [4]. The mixing layer interacts with the right-hand wall of the recess, as a result of which a pressure wave is formed, which propagates upstream within the recess and, upon reaching the left-hand wall, is reflected from it and travels in the opposite direction. In Fig. 6 we give a graph of the pressure variation as a function of time at the topmost calculation point on the right-hand wall of the cavity. In Fig. 4 we show graphs of the pressure distribution on the vertical walls of the cavity (dashed lines for the right-hand wall and solid lines for the left-hand wall) for the times $t_1 = 260$ and $t_3 = 270$ designated in Fig. 6. Strong return flow occurs in the interior of the cavity (see Fig. 7). The recirculation configuration of the field may be seen; the center of the recirculation region is located near the upper corner point of the back wall of the cavity, in agreement with the data of [3].

The period of the pressure oscillations, which are weakly damped, that develop in the cavity is about $T_p \approx 19.7$ (see Fig. 6), i.e., their frequency is $f_p \approx 0.0507$. Rossiter's formula for estimating the possible frequencies f of oscillations in a cavity was given in [3]:

$$f = mu_\infty/(L(1/k + 1/a)), \tag{4}$$

where m is the mode number; $c_1/u_\infty = k$ is the velocity of the forward propagating wave; $a = c_2/u_\infty = (1 + 0.2M_\infty^2)^{1/2}/M_\infty$ is the velocity of the backward wave. For the conditions of the problem under consideration, $k \approx 0.5$, ≈ 1.15, and for m = 1 Rossiter's formula gives a period $T \approx 18.9$ or a frequency $f \approx 0.0528$.

A semiempirical method of calculating the frequencies of discrete components of the spectrum of pressure pulsations in a cavity has been given in [4]. According to the data of [1], the Strouhal number for the lowest pulsation frequency f_0 at M = 1.35 is $Sh = fL/u_\infty = 0.28$. In the numerical experiment, $Sh \approx 0.30$.

The above calculations show that using a KCDS with correction for the calculation of laminar detached flow of a viscous compressible gas enables one to obtain a reliable qualitative picture of the flow and to calculate with acceptable accuracy some quantitative characteristics of the flow, even in the nonsteady case, which is complicated to simulate.

1217

NOTATION

h_x, h_y, grid steps; ρ, density; u, v, velocity components; p, pressure; ε, internal energy; $E = \rho(\varepsilon + 0.5(u^2 + v^2))$, total energy; μ, viscosity coefficient; $c = \sqrt{\gamma(\gamma-1)\varepsilon}$ speed of sound; Re, Reynolds number; Pr, Prandtl number; γ, adiabatic index; T_w, all temperature; T_e, equilibrium wall temperature; M, Mach number; δ, thickness of the boundary layer; q, heat flux at the wall. Indices: ∞, parameters in the undisturbed oncoming stream; $\overset{0}{x}$, $\bar{x}$, x, ($\overset{0}{y}$, $\bar{y}$, y), central, left-hand, and right-hand difference derivatives with respect to x (and to y), respectively.

LITERATURE CITED

1. P. K. Chang, Separation of Flow, Pergamon Press, Oxford—New York (1970).
2. A. N. Antonov, V. M. Kuptsov, and V. V. Komarov, Pressure Pulsations in Jet and Detached Flows [in Russian], Moscow (1990).
3. W. L. Hankey and J. S. Shang, AIAA J., 18, No. 1 (1980).
4. A. N. Antonov, A. N. Vishnyakov, and S. P. Shalaev, Zh. Prikl. Mekh. Tekh. Fiz., 7, No. 2, 89-98 (1981).
5. S. N. Sinha, A. K. Gupta, and M. M. Oberai, AIAA J., 20, No. 3, 370-375 (1982).
6. D. Brandeis, Aerokosm. Tekh., 1, No. 2, 45-53 (1983).
7. I. G. Makarov, Izv. Akad. Nauk SSSR, Mekh. Zhidk. Gaza, No. 2, 173-175 (1989).
8. N. L. Zaugol'nikov, M. A. Koval', and A. I. Shvets, Izv. Nauk SSSR, Mekh. Zhidk. Gaza, No. 2, 121-127 (1990).
9. I. A. Graur, T. G. Elizarova, and B. N. Chetverushkin, "Kinetically consistent difference schemes for calculating heat transfer in supersonic gas-dynamic streams," Preprint No. 90, Inst. Prikl. Mat. Im. Keldysha, Akad. Nauk SSSR, Moscow (1988).
10. T. G. Elizarova and B. N. Chetverushkin, Zh. Vychisl. Mat. Mat. Fiz., 28, No. 11, 695-710 (1988).
11. L. G. Loitsyanskii, Mechanics of Liquids and Gases, Pergamon Press, Oxford—New York (1966).

DYNAMICS OF A BOUNDED GAS CAVITY IN A PIPE

V. G. Kinelev and P. M. Shkapov

UDC 532.529.5

The dynamics of a gas cavity formed in a pipe in the zone of flow separation behind a cavitating body, and bounded by a diaphragm mounted at a pipeline exit, is considered. A mathematical model is proposed, on the basis of which the stability of the flow under consideration is investigated.

At present, more emphasis is being placed on the investigation of the dynamics of cavitation flows in pipes and flow elements of hydraulic systems. Of particular interest are flows with a developed connected cavity that is formed in the zones of flow separation behind the bluff elements of the structure or by special cavitating bodies. In these regions of flow with reduced pressure, a diffusive liberation of the dissolved gas or a buildup of dispersed gas bubbles that separate from the incoming flow takes place. When a certain critical cavitation number is realized, this results in the formation of a single cavity — a connected cavity with a sharply expressed gas—liquid interface. The adjustment of the dimensions of the middle sections of a cavitating body and a pipe, the blowing of the gas in the region of separation, as well as flow swirl, either natural or applied, affect substantially the intensity of these processes. When the cavitation number diminishes, the cavity dimensions increase along the flow, and flow lines at its interface tend to become parallel to each other and to the pipe walls in the limit [1-3].